PHYSICAL REVIEW B **70**, 134106 (2004)

Spiral chain structure of high pressure selenium-II′ and sulfur-II from powder x-ray diffraction

Hiroshi Fujihisa,[1] Yuichi Akahama,[2] Haruki Kawamura,[2] Hiroshi Yamawaki,[1] Mami Sakashita,[1] Takahiro Yamada,[1]
Kazumasa Honda,[1] and Tristan Le Bihan[3]
[1]*National Institute of Advanced Industrial Science and Technology (AIST), 1-1-1 Higashi, Tsukuba, Ibaraki 305-8565, Japan*
[2]*Graduate School of Material Science, University of Hyogo, 3-2-1 Koto, Kamigohri, Akohgun, Hyogo 678-1297, Japan*
[3]*European Synchrotron Radiation Facility (ESRF), BP220, F38043 Grenoble, France*
(Received 9 April 2004; revised manuscript received 2 June 2004; published 21 October 2004)

The structure of high pressure phases, selenium-II′ (Se-II′) and sulfur-II (S-II), for α-Se$_8$ (monoclinic Se-I) and α-S$_8$ (orthorhombic S-I) was studied by powder x-ray diffraction experiments. Se-II′ and S-II were found to be isostructural and to belong to the tetragonal space group $I4_1/acd$, which is made up of 16 atoms in the unit cell. The structure consisted of unique spiral chains with both 4_1 and 4_3 screws. The results confirmed that the structure sequence of the pressure-induced phase transitions for the group VIb elements depended on the initial molecular form. The chemical bonds of the phases are also discussed from the interatomic distances that were obtained.

DOI: 10.1103/PhysRevB.70.134106 PACS number(s): 61.50.Ks, 62.50.+p, 64.70.Kb, 61.10.Nz

I. INTRODUCTION

Sulfur, selenium, and tellurium of the group VIb elements form many polymorphs at ambient pressure and temperature. The α forms are typical molecular crystals consisting of S$_8$ (Ref. 1) and Se$_8$ (Ref. 2) ring molecules and are often called orthorhombic S-I (a stable form) and monoclinic Se-I (a metastable form). Amorphization takes place at 20 GPa (Ref. 3) when compressing S-I at room temperature, and recrystallization occurs around 35 GPa with further compression. This phase is called S-II (Ref. 4) and has an electrical property of being a semiconductor.[5] The structure of S-II is not known. This phase transforms to an orthorhombic S-III (4) with a puckered layer structure at 83 GPa and further to a β-Po structure of S-IV (Ref. 6) at 162 GPa. From the electrical and optical studies, S-III and IV have been reported to be metallic[5] and become a superconductor at low temperature.[7,8] For monoclinic Se-I at room temperature, a crystalline Se-II′ appears directly at 10 GPa without showing amorphization.[9] Its structure is also unknown, although many investigators have observed the transition from a semiconductor to a metal, which corresponds to the structure transition.[10–15] By further compression, it undergoes a transition to Se-IV (orthorhombic) with the puckered layer structure[9] at 33 GPa. Recently, the structure of Se-IV was reported to be incommensurately modulated.[16] Our recent Raman studies have suggested that Se-II′ is isostructural with S-II and does not follow the sequence of the pressure-induced structure transitions of trigonal-Se with a spiral chain structure,[17] which is a stable form for Se.

Our objective is to investigate the crystal structures of S-II and Se-II′. They are essential for understanding the metallization process and how the ring molecules change to the layered structure. They are of great importance, but their structures are not known. From this reason, we performed powder x-ray diffraction experiments and were able to succeed in determining their structures.

II. EXPERIMENT

A powder sample of S-I with a stated purity of 99.9999% was put in a diamond anvil cell (DAC) used for pressure generation and loaded to 48 GPa at 77 K to avoid recrystallization. A single crystal of monoclinic Se-I was softly ground to avoid oxidation and the transition to trigonal Se. Then the powder was mounted immediately into a gasket hole. Pressure transmitting media were not used for fear of a chemical reaction with a fragment of a dissociated molecule, since the transitions from the molecular phase to the higher pressure phases are related to a molecular dissociation. The pressures were determined with the ruby pressure scale.[18] Angle-dispersive powder x-ray diffraction experiments were performed on three synchrotron facilities with an image plate detector (IP) at room temperature. The two-dimensional diffraction images were integrated by the software PIP (Powder pattern analyzer for IP) into 2θ-intensity patterns.[19]

An experiment (run 1) was performed on Se-II′ on the BL-10XU beam line at the SPring-8. The x-ray beam was monochromatized to a wavelength of 0.4964 Å and was collimated to a 40-μm square. Figure 1 shows an example of the raw diffraction pattern at 15.3 GPa recorded on an IP. A second experiment (run 2) was performed on Se-II′ on the BL-18A beam line at the Photon Factory with a 0.4860-Å

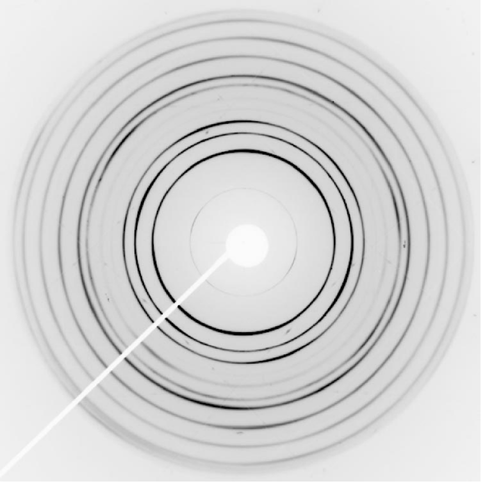

FIG. 1. Powder diffraction image of Se-II′ at 15.3 GPa recorded on an image plate.

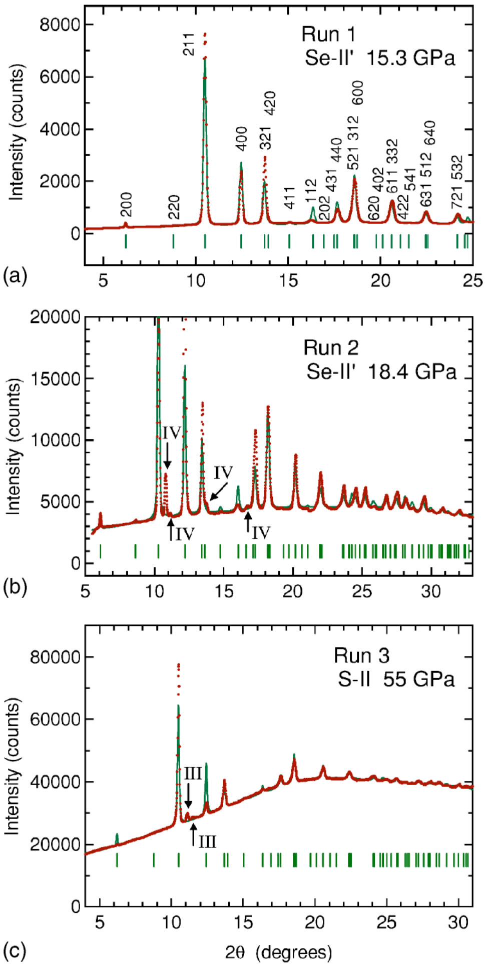

FIG. 2. (Color online) Diffraction patterns and Rietveld fits of (a) run 1 for Se-II′ at 15.3 GPa, (b) run 2 for Se-II′ at 18.4 GPa, and (c) run 3 for S-II at 55 GPa. The arrows marked IV in (b) represent the peaks from the higher pressure phase of Se-IV. The arrows marked III in (c) represent the peaks from the higher pressure phase of S-III. Typical R factors of the Rietveld fit were R_{wp} $=12\%$ and $R_p=7\%$.

and an 80-μm diameter beam. A third experiment (run 3) was performed on S-II on the ID-30 beam line at the European Synchrotron Radiation Facility (ESRF) with a 0.4246-Å and a 25-μm square beam. When the sulfur was compressed normally, the background level of the S-II pattern became very high from passing through the amorphous phase. Therefore, the powder was compressed once to the S-III region beyond 84 GPa, then downloaded to the S-II region.

III. ANALYSIS

Since the 15.3-GPa data in run 1 gave the smoothest Debye-Scherrer rings with no contamination peaks, an indexing was done with this pattern. All of the peaks were successfully indexed with a tetragonal cell as shown in Fig. 2(a). The cell was found to have an I-centered symmetry based on the entire extinction rule ($hkl{:}h+k+l=2n$). Additional disappearances of the 110 and 011 reflections uniquely determined its space group to be D_{4h}^{20}—$I4_1/acd$ (no.142) which has an extinction rule of $hk0{:}h,k=2n$ and $0kl{:}k,l=2n$. By comparing the volumes of the cell to that of Se-IV, the cell was allowed to contain 16 selenium atoms. Only the 16 f Wyckoff site of this space group, which has the extinction of $hkl{:}l=2n+1$ or $2h+l=4n$, could match the disappearances of the 202 and 402 peaks, and the appearances of the 211 and 321 peaks. Thus a Rietveld refinement with the 16 f $(x,x,1/4)$ site of origin choice 1 was successfully made, as shown by a solid curve in Fig. 2(a). The cell and atomic parameters were refined to be $a=9.148\pm0.001$ Å, $c=3.626\pm0.001$ Å, and $x=0.132\pm0.001$. The axial ratio c/a was 0.3964 ± 0.0002, and the volume per one selenium atom became 18.965 ± 0.009 Å^3.

The tetragonal $I4_1/acd$ structure was also applied to a run 2 pattern at 18.4 GPa. This pattern had a higher diffraction angle data up to 33° and provided more reliable lattice parameters. By a Rietvevld fit shown in Fig. 2(b), the cell parameters were refined to be $a=9.148\pm0.001$ Å and $c=3.615\pm0.001$ Å. Since the Debye-Scherrer rings for run 2 did not have uniform intensity due to the preferred orientation effect, the atomic parameter x was fixed to 0.132 of the value obtained in run 1. The axial ratio and the atomic volume were determined to be 0.3952 ± 0.0002 and 18.908 ± 0.009 Å^3. The higher angle data from 25° to 33° which could not be obtained from the data of run 1 could be fitted by this tetragonal structure. All the unassigned peaks marked IV in Fig. 2(b) were found to belong to those from the higher pressure phase Se-IV. Previous patterns from Ref. 9 which reported the first observation of Se-II′ could also be fitted by this tetragonal and Se-IV structures.

The diffraction pattern of S-II at 55 GPa was quite similar to that of Se-II′ and showed the same structure. A Rietveld analysis, shown in Fig. 2(c), revealed that its structure also belongs to the same tetragonal space group $I4_1/acd$, which is made up of 16 sulfur atoms in the unit cell. The cell and atomic parameters were refined to be $a=7.841\pm0.001$ Å, $c=3.100\pm0.001$ Å, and $x=0.136\pm0.001$. The axial ratio and the atomic volume were determined to be 0.3953 ± 0.0002 and 11.912 ± 0.007 Å^3.

IV. DISCUSSION

Figure 3(a) displays the tetragonal $I4_1/acd$ structures of Se-II′ determined at 15.3 GPa. A spiral chain can be seen along the c axis. A special feature of this tetragonal structure is the coexistence of both the 4_1-screw and the 4_3-screw axes. That is, the bottom-left chain in Fig. 3(b) corresponds to the right screw. The adjacent bottom-right and top-left chains correspond to the left screws. For the group-VIb elements, this spiral chain structure is commonly seen in trigonal-Te, trigonal-Se as shown in Fig. 3(c), and the high-pressure high-temperature phase of sulfur (high-PT phase).[20] However, all of those crystals only have a 3_1- or a 3_2-screw chain. Namely, the coexistence of both screw chains occurs under high pressure.

A pitch of the spiral chain corresponds to a length of the c axis for each case of Se-II′, trigonal-Se, S-II, and sulfur high-PT phase. The pitch for Se-II′ (3.626 Å at 15.3 GPa) was 27% shorter than that for trigonal-Se [4.954 Å at 1 bar (Ref. 21)]. The pitch for S-II (3.100 Å at 55 GPa) was 28%

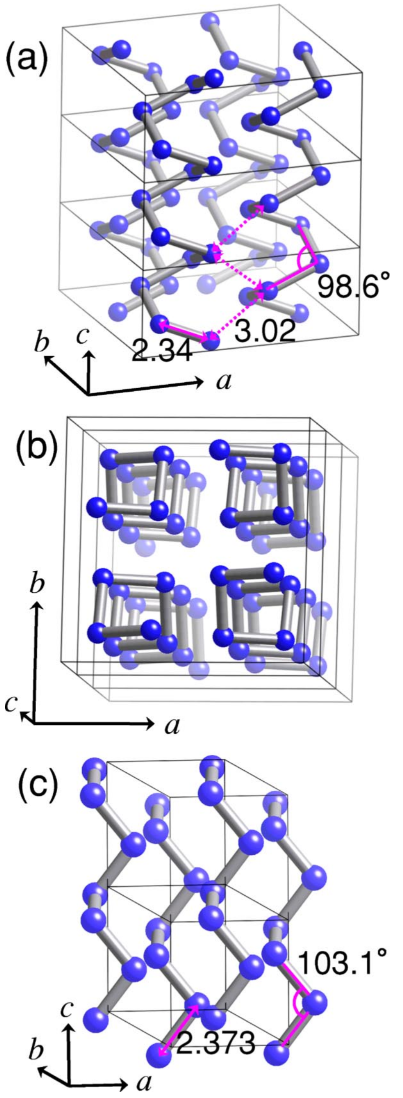

FIG. 3. (Color online) (a) The triple cells along the *c* axis of the tetragonal $I4_1/acd$ structures for Se-II′ at 15.3 GPa. (b) Top view of the *ab* plane of the same cells. (c) The double cells along the *c* axis of the trigonal-Se at 1 bar (Ref. 21) for comparison. The first-nearest-neighbor Se-Se distance was depicted with sticks in each figure. The second-nearest-neighbor distance was drawn with dashed lines.

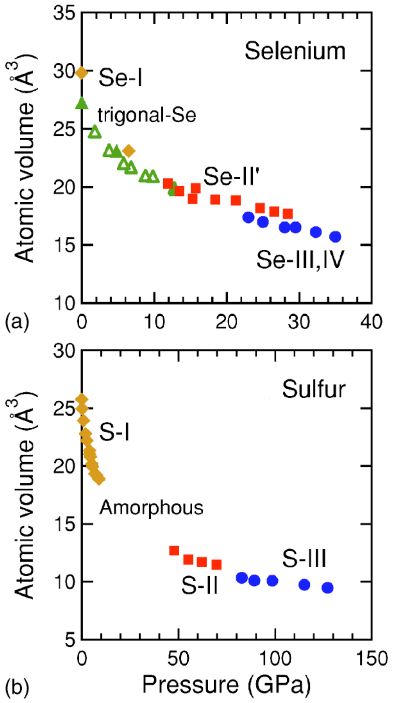

FIG. 4. (Color online) Pressure versus atomic volume for (a) selenium and (b) sulfur. Open and closed triangles represent the data for trigonal-Se from Refs. 25 and 26. Diamonds show the data for the starting molecular phases of Se-I (Ref. 9) and S-I (present work). Squares represent the tetragonal Se-II′ and S-II data determined by this work. Circles represent the data for the puckered layer phases of Se-III (Ref. 27), Se-IV (Ref. 27), and S-III (present work).

shorter than that of the high-PT phase [4.302 Å at 3 GPa and 400 °C (Ref. 20)]. The ratios of the pitches were almost the same for both cases of selenium and sulfur. The intrachain bond angles for Se-II′ (98.6°) and S-II (99.1°) were also similar, but were smaller than those for trigonal-Se [103.1° (Ref. 21)] and sulfur high-PT phase [102.7° and 101.7° (Ref. 20)].

The first-nearest distance of Se-II′, corresponding to the intrachain distance, was determined by the Rietveld analysis to be 2.34±0.01 Å at 15.3 GPa, as shown in Fig. 3(a). This value is almost the same as the averaged intramolecular distance of monoclinic Se-I [2.336 Å (Ref. 2)] and the intrachain distance of trigonal-Se [2.373 Å (Ref. 21)], as shown in Fig. 3(c). This is also true for S-II (1.95 Å at 55 GPa), S-I [2.041 Å average at 1 bar (Ref. 1)], and the high-PT phase [2.070 Å and 2.096 Å at 3 GPa and 400 °C (Ref. 20)] relation. These facts show that the intrachain bond is covalent and remains strong.

The second-nearest distances, corresponding to the closest interchain distances, were determined to be 3.02±0.01 Å at 15.3 GPa, as shown with dashed lines in Fig. 3(a) and are important for discussing the electrical property. The intermolecular distance of monoclinic Se-I at 1 bar (3.48 Å average[2]) is still longer than twice the selenium constant energy radius [$2r_A^*=3.16$ Å (Ref. 22)], which is a criterion for the existence of the overlapping of the molecular orbitals or of the covalent bond formation. This means the intermolecular interaction is weak and its electrical property is an insulator at ambient pressure. After the phase transition to Se-II′, the closest interchain distance became 3.02 Å at a pressure of 15.3 GPa as shown in Fig. 3(a), below the critical value of 3.16 Å. At this pressure, the interchain interaction should strengthen the forwarding metallic state. This theory also applies for sulfur. The intermolecular distance of S-I at 1 bar (3.31 Å average[1]) is still longer than twice the sulfur constant energy radius [$2r_A^*=2.92$ Å (Ref. 22)]. The closest interchain distance of S-II decreases to 2.63 Å at 55 GPa. These results agree with the electrical behaviors for selenium and sulfur that the present tetragonal phases exist as an intermediate state between the insulator and the metal.

Figure 4(a) displays the pressure dependence of the volume per one atom for various selenium phases. The volume of trigonal-Se (open and closed triangles) is smaller than that of monoclinic Se-I (diamonds). This corresponds to trigonal-Se (a stable phase) having a higher packing index and to monoclinic Se-I (a metastable phase) having large spaces between the Se_8 molecules. The transition to Se-II′ is accompanied by molecular dissociation. As a result, such spaces decreased and the volume became comparable to that of trigonal Se. The transition from Se-II′ to Se-IV was irreversible, and Se-IV transformed into a trigonal Se with decreasing pressure. The pressure dependence of the volume of sulfur is also shown in Fig. 4(b). A volume jump was not recognized for sulfur, since the volume of the amorphous phase was not known. However, the volume of S-II seemed to be consistent compared with that of S-III. The transition between S-II to S-III was reversible. In a pressure releasing cycle, S-II was reproduced around 59 GPa. Therefore, the S-II phase can be considered to be a stable high-pressure phase.

In this study, the pressure-induced dissociation of Se_8 and S_8 ring molecules was revealed from the structural aspect. Up to now, the Se-II′ phase has been proposed to be isostructural with S-II and did not follow the sequence of the pressure-induced structure transitions of a trigonal Se with a spiral chain structure.[17] The present study also confirmed this suggestion.

The tetragonal structure that was determined by this study has not been seen in other elements. However, we can find a similar structure with the same space group in a molecular crystal of hydrogen sulfide (H_2S). In a high-pressure phase IV appearing above 12 GPa, the sulfur atoms of H_2S molecules contact each other directly and form the same spiral chains[23] with the 4_1-screw and the 4_3-screw axes along its c axis. The interchains are connected by hydrogen bonds. For Se-II′ and S-II, there may be other kinds of attractive forces to stabilize this structure. After a molecular dissociation of H_2S above 27 GPa, the dissociated sulfur atoms behave like elemental sulfur and form the S-II structure.[24] The diffraction pattern in this reference has now been identified by the tetragonal structure determined in this study.

ACKNOWLEDGMENTS

The present work was carried out with the approval of the Photon Factory Program Advisory Committee (Proposal No. 94G113), SPring-8 (No. 2002A0189), and ESRF (No. 1998HS1076).

---

[1] G. S. Pawley and R. P. Rinaldi, Acta Crystallogr., Sect. B: Struct. Crystallogr. Cryst. Chem. **28**, 3605 (1972).

[2] P. Cherin and P. Unger, Acta Crystallogr., Sect. B: Struct. Crystallogr. Cryst. Chem. **28**, 313 (1972).

[3] H. Luo and A. L. Ruoff, Phys. Rev. B **48**, 569 (1993).

[4] Y. Akahama, M. Kobayashi, and H. Kawamura, Phys. Rev. B **48**, 6862 (1993).

[5] H. Luo, S. Desgreniers, Y. K. Vohra, and A. L. Ruoff, Phys. Rev. Lett. **67**, 2998 (1991).

[6] H. Luo, R. G. Greene, and A. L. Ruoff, Phys. Rev. Lett. **71**, 2943 (1993).

[7] S. Kometani, M. I. Eremets, K. Shimizu, M. Kobayashi, and K. Amaya, J. Phys. Soc. Jpn. **66**, 2564 (1997).

[8] E. Gregoryanz, V. V. Struzhkin, R. J. Hemley, M. I. Eremets, H. K. Mao, and Y. A. Timofeev, Phys. Rev. B **65**, 064504 (2002).

[9] Y. Akahama, M. Kobayashi, and H. Kawamura, Phys. Rev. B **56**, 5027 (1997).

[10] A. S. Balchan and H. G. Drickamer, J. Chem. Phys. **34**, 1948 (1961).

[11] B. M. Riggleman and H. G. Drickamer, J. Chem. Phys. **38**, 2721 (1963).

[12] J. Wittig, J. Chem. Phys. **58**, 2220 (1973).

[13] F. P. Bundy and K. J. Dunn, J. Chem. Phys. **71**, 1550 (1979).

[14] Y. Akahama, M. Kobayashi, and H. Kawamura, Solid State Commun. **84**, 803 (1992).

[15] Y. Ohmasa, I. Yamamoto, M. Yao, and H. Endo, J. Phys. Soc. Jpn. **64**, 4766 (1995).

[16] C. Hejny and M. I. McMahon, Phys. Rev. Lett. **91**, 215502 (2003).

[17] Y. Akahama and H. Kawamura, in *Proceedings of 43rd High Pressure Conference of Japan*, Matsuyama, Japan 2002 (The Japan Society of High Pressure Science and Technology, Japan, 2002), p. 132.

[18] H. K. Mao, P. M. Bell, J. W. Shaner, and D. J. Steinberg, J. Appl. Phys. **49**, 3276 (1978).

[19] O. Shimomura, K. Takemura, H. Fujihisa, Y. Fujii, Y. Ohishi, T. Kikegawa, Y. Amemiya, and T. Matsushita, Rev. Sci. Instrum. **63**, 967 (1992).

[20] W. A. Crichton, G. B. M. Vaughan, and M. Mezouar, Z. Kristallogr. **216**, 417 (2001).

[21] P. Cherin and P. Unger, Inorg. Chem. **6**, 1589 (1967).

[22] M. L. Huggins, J. Am. Chem. Soc. **75**, 4126 (1953).

[23] H. Fujihisa, H. Yamawaki, M. Sakashita, K. Aoki, S. Sasaki, and H. Shimizu, Phys. Rev. B **57**, 2651 (1998).

[24] H. Fujihisa, H. Yamawaki, M. Sakashita, A. Nakayama, T. Yamada, and K. Aoki, Phys. Rev. B **69**, 214102 (2004).

[25] K. Nagata and Y. Miyamoto, in *High Pressure Research on Solids*, edited by M. Seno *et al.* (Elsevier Science B. V. and The Society of Materials Science, Japan, 1995), pp. 19–38.

[26] Y. Akahama, M. Kobayashi, and H. Kawamura, Solid State Commun. **83**, 269 (1992).

[27] Y. Akahama, M. Kobayashi, and H. Kawamura, Phys. Rev. B **47**, 20 (1993).